Geophysical Research Letters

RESEARCH LETTER
10.1029/2022GL098599

Dynamic Steady State in Coastal Aquifers Is Driven by Multi-Scale Cyclical Processes, Controlled by Aquifer Storativity

Anner Paldor[1], Ryan S. Frederiks[1], and Holly A. Michael[1,2]

[1]Department of Earth Sciences, University of Delaware, Newark, DE, USA, [2]Department of Civil and Environmental Engineering, University of Delaware, Newark, DE, USA

Key Points:

- Average salinities in coastal aquifers are affected by low-frequency cyclical changes in sea level (SL)
- High-frequency cyclical forcings generate episodic discrepancies in salinity when modeled with and without considering these processes
- Under these multi-scale fluctuations in SL, dynamic steady states of coastal aquifers are affected by aquifer storage properties

Correspondence to:
H. A. Michael,
hmichael@udel.edu

Citation:
Paldor, A., Frederiks, R. S., & Michael, H. A. (2022). Dynamic steady state in coastal aquifers is driven by multi-scale cyclical processes, controlled by aquifer storativity. *Geophysical Research Letters*, *49*, e2022GL098599. https://doi.org/10.1029/2022GL098599

Received 6 MAR 2022
Accepted 20 MAY 2022

Author Contributions:
Conceptualization: Anner Paldor, Ryan S. Frederiks, Holly A. Michael
Formal analysis: Anner Paldor, Ryan S. Frederiks, Holly A. Michael
Funding acquisition: Holly A. Michael
Investigation: Anner Paldor, Ryan S. Frederiks, Holly A. Michael
Methodology: Anner Paldor, Ryan S. Frederiks
Project Administration: Anner Paldor, Holly A. Michael
Resources: Holly A. Michael
Supervision: Holly A. Michael
Validation: Holly A. Michael
Visualization: Anner Paldor
Writing – original draft: Anner Paldor
Writing – review & editing: Ryan S. Frederiks, Holly A. Michael

Abstract Coastal aquifers supply freshwater to nearly half the global population, yet they are threatened by salinization. Salinities are typically estimated assuming steady-state, neglecting the effect of cyclical forcings on average salinity distributions. Here, numerical modeling is used to test this assumption. Multi-scale fluctuations in sea level (SL) are simulated, from tides to glacial cycles. Results show that high-frequency fluctuations alter average salinities compared with the steady-state distribution produced by average SL. Low-frequency forcing generates discrepancies between present-day salinities estimated with and without considering the cyclical forcing due to overshoot effects. This implies that salinities in coastal aquifers may be erroneously estimated when assuming steady-state conditions, since present distributions are likely part of a dynamic steady state that includes forcing on multiple timescales. Further, typically neglected aquifer storage characteristics can strongly control average salinity distributions. This has important implications for managing vulnerable coastal groundwater resources and for calibration of hydrogeological models.

Plain Language Summary Coastal communities rely heavily on groundwater for freshwater supply, and the primary risk for this vital resource is salinization. Multiple processes in the ocean-land interface control the salinity of coastal aquifers, and assessments of salinities typically neglect some of these processes. In this work, we show that some of the typically neglected processes may be responsible for large-scale, systematic discrepancies between actual and estimated salinities. This has important implications for the assessment of risks to coastal groundwater reservoirs and for the long-term management of these resources.

1. Introduction

Groundwater is commonly the primary source of freshwater in coastal communities and plays a significant role in human resilience to increasing water stresses. The state of coastal aquifers (head and salinity) is highly variable, and the interface with the ocean exposes them to a multitude of salinization processes that compromise freshwater supply (Michael et al., 2017). These salinization mechanisms can occur on multiple spatio-temporal scales, and the interplay between them often renders their detection and isolation impossible. Therefore, coastal aquifers are rarely in true steady state, but in a dynamic steady state, under which salinities and heads fluctuate on time scales ranging from seconds to thousands of years. The dynamic steady state of aquifers, in which conditions fluctuate around an average, is controlled by their hydraulic properties, which dictate the response of the aquifer to cyclical processes that cause head and salinity to fluctuate.

Management of coastal aquifers relies on knowing the salinity distributions, and this is particularly important in places with scarce water resources. Monitoring the salinity of coastal aquifers is difficult because it requires installation of observation wells that intersect with the subsurface transition zone between saline and fresh groundwater, the location of which is often unknown. Furthermore, this transition zone is often heterogeneous, making it even harder to delineate via direct measurements. Therefore, coastal hydrogeologists commonly rely on modeling to predict the current and future location of the transition zone, and design management strategies accordingly.

An added complication is that coastal systems are subjected to cyclical forcings that may induce changes in salinity over timescales from seconds (waves) to thousands of years (glacial cycles). Due to the diversity of the spatio-temporal scales of cyclical forcings, hydrogeologists often estimate the state of coastal aquifers assuming a steady sea level (SL), which could be the average SL of a periodic force (e.g., waves, tides), or the SL corresponding to modern calm conditions, ignoring cyclical forcings that are not around the present-day mean SL (e.g., storms, glacial cycles). It has recently been recognized that for long-term and large-amplitude fluctuations such as

glacial changes in SL, equilibration periods can be very long and salinity may be in a transient state, particularly for continental shelf-scale confined aquifer systems (Cohen et al., 2010; Micallef et al., 2020; Paldor et al., 2019; Post et al., 2013), invalidating the steady-state assumption. However, only a few studies have investigated the extent to which this may occur, and it is rarely considered in management of shallower unconfined systems. While it has been shown that wave runup has a significant impact on the salinity distribution of barrier islands (Nielsen, 1999), and that wave and tidal fluctuations can induce an upper saline plume (Robinson et al., 2007; Xin et al., 2010), the impact of these processes on the location of the interface at larger scales has not been investigated. At regional scales, shorter-term processes such as waves and tides that typically fluctuate around the mean with a relatively low amplitude (on the order of 10^{-1}–10^{0} m) are widely assumed to have negligible impact on the larger-scale salinity distribution. Thus it is presumed reasonable to estimate the average salinity distribution of an aquifer in dynamic steady state based on present-day average SL.

Here we challenge these widely held assumptions and examine the impact of natural periodic forcing over multiple spatio-temporal scales on the dynamic steady state of coastal aquifers. We further explore the effect of aquifer storativity, S (by considering changes in the specific storage—S_s) on these dynamic steady states. Storativity is typically considered when modeling transient processes (e.g., Chang et al., 2011; Levanon et al., 2016; Watson et al., 2010; Xu et al., 2018), but is often overlooked in hydrogeologic modeling that neglects transient forcing, because steady-state solutions to the groundwater flow equation do not include S. The processes simulated here range from tidal fluctuations (diurnal time scale and a ∼1 m change in SL), to glacial cycles (∼10^4 yr time scale with SL changes on the order of ∼50 m).

2. Methods

This study uses 2D generalized models developed in HydroGeoSphere (Therrien et al., 2010), an integrated hydrologic model that couples surface and subsurface flow and salt transport, including variable-density flow. Model dimensions and spatial and temporal discretization varied based on the process simulated. For each process, two values of specific storage were simulated: $S_s = 1 \times 10^{-1}$ m^{-1} and $S_s = 1 \times 10^{-4}$ m^{-1}. We note here that S_s is an aquifer characteristic that depends on the compressibility of the porous material. A value of $S_s = 1 \times 10^{-1}$ is therefore not necessarily representative of real aquifers. However, as the motivation is to study differences in the response of coastal aquifers to cyclical changes in SL, and since the numerical implementation in HydroGeoSphere only allows adjustment of S_s and porosity, it is insightful to adopt these two values of S_s to represent differences in the overall storativity (S) of aquifers. Since changing the porosity would affect the linear flow velocity and thus the solute transport solution, we simulated changes in storativity by adjusting S_s. Hydraulic conductivity was set to $K = 5$ md^{-1} for all simulations. In nature, K may decrease with depth in the aquifer, but for simplicity we consider a uniform K. In all simulations, porosity was set to 0.3, longitudinal and transverse dispersivities were 10 and 1 m (respectively), and freshwater and seawater densities were set to 1,000 and 1,025 kg·m^{-3} (respectively). The periodic processes that were tested are listed below in increasing order of the period:

1. Tidal pumping (∼0.5 day period, amplitude on the order of 1 m) (Levanon et al., 2017).
2. Storm-surge inundations (∼10 year period reflected as recurrence time for surges on the order of 3 m) (Tebaldi et al., 2012).
3. Glacial-scale, sea-level fluctuations (∼1·10^4 yr period, with SL changes on the order of 50 m) (Person et al., 2003).

For each process, a specific model domain was configured to accommodate the tested amplitude of fluctuations. This means that the model length (L in Figure 1) and thickness (H) were increased with the vertical amplitude of the tested process. Figure 1 shows an example of a model domain with the adopted boundary conditions. Each of the 3 sets of simulations was initially run to steady state with a constant SL. The boundary conditions were no-flow at the bottom and the offshore vertical boundary, constant flux on the landside (blue dots in Figure 1) with freshwater salinity ($C = 0$), and on the surface node corresponding to the maximum seaward extent of the model (red circle in Figure 1) a prescribed head with seawater salinity ($C = 1$). The constant head was prescribed to facilitate comparisons between transient and steady-state simulations for each given process, as they would have been simulated without the respective sea-level changes: For the tides, this was the average of the tidal fluctuations (Figure 1a); For the storm surges, this is the minimum value, corresponding to calm conditions (Figure 1b); For the glacial sea-level changes, this is the maximum of the sine function, as it is the current state

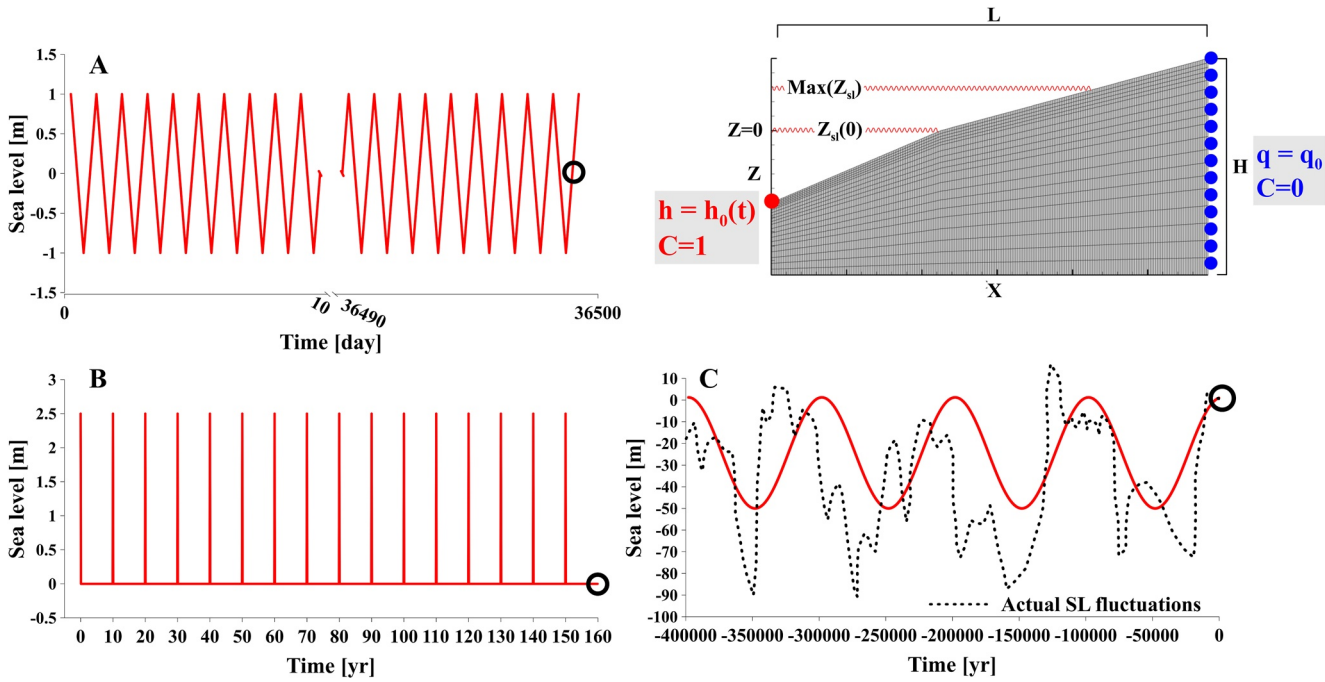

Figure 1. Model setup and (a–c) boundary conditions. Z_{sl} denotes the elevation of sea level (SL). Specific dimensions (H, L) and the seaside boundary condition (h_0) were varied among simulated processes: (a) Tidal fluctuations (Levanon et al., 2017), (b) Storm-surge inundation (Tebaldi et al., 2012), (c) Glacial-scale changes in SL as simulated here (red curve) and the reconstructed paleo sea levels in black dashed line (Person et al., 2003). Red/blue points in the upper-right panel are the model nodes where SL/recharge boundary conditions were applied, respectively. Black circles mark the sampled times for the plots in Figure 3.

based on reconstruction of paleo sea levels (Person et al., 2003) (Figure 1c). The result of each steady-state simulation was used as the initial condition for the subsequent, transient simulation. While these processes are likely confounded in reality by accompanying changes in the hydrologic regime (e.g., changes in precipitation during storm surges), this study focuses on the different forcings related to SL fluctuations, and it is therefore informative to isolate this component.

The transient processes were simulated by assigning a time-dependent SL boundary condition (Figure 1). SL was varied by changing the assigned head on the surface node at the seaside, with the specific function ($h_0(t)$) depending on the simulated process (Figure 1a–1c). For the tidal simulations, a piecewise linear change between high and low tide was applied (Figure 1a). This was set to balance model accuracy with reasonable runtimes, but it is noted that a sine function would be more realistic if the number of stress periods and runtime were not an issue. The surface water domain in HydroGeoSphere allows for inundation and draining/infiltration/discharge along the model surface in response to changing SL without constraining the subsurface nodes. The landside wall (blue dots in Figure 1) was a fixed freshwater flux with a constant value ($q_0 = 0.002$ md^{-1}). This allows the inland head value to adjust in response to sea-level changes.

To quantify the differences between steady-state simulations (i.e., $h_0 = \text{const.}$) and dynamic steady state simulations with cyclical forcings ($h_0 = f(t)$), we use two model outputs. The first is the location and distribution of the subsurface mixing zone, defined between the 10% ($C = 0.1$) and the 90% ($C = 0.9$) seawater salinity contours. The second metric is the mass of salt in the aquifer normalized by the steady-state value:

$$\overline{\text{SM}}(t) = \frac{\text{SM}(t)}{\text{SM}(0)} \tag{1}$$

Simulated values of $\overline{\text{SM}} > 1$ mean that the aquifer is more salinized compared with the steady state (SM(0)). The minimum possible value of $\overline{\text{SM}}$ is zero, meaning that the system is entirely flushed out of salt (SM(t) = 0).

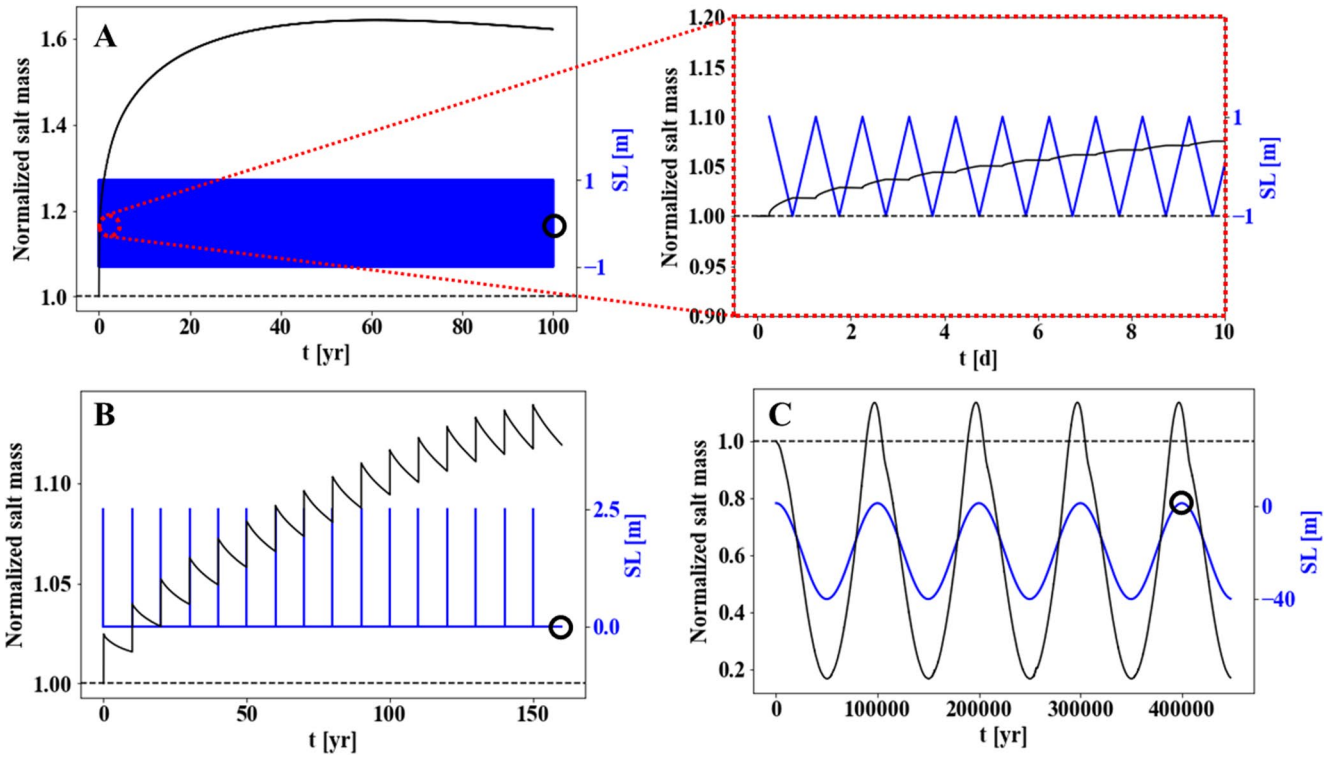

Figure 2. Normalized salt mass $\overline{SM}$ (black curves) and the applied BC (blue curves) for the three simulated processes: (a) Tides; (b) Surges; (c) Glacial-scale fluctuations in sea level (SL). Black circles mark the times plotted in Figure 3 (corresponding with the black circles marked on Figure 1). The black dashed lines are $\overline{SM} = 1$, which is the initial (steady state) value for the transient simulations. In panel a (tides) the BC curve appears as a blue rectangle because of the scale (diurnal fluctuations over 100 years period, the inset in red shows a detailed curve for the first 10 days).

3. Results

3.1. Dynamic-Steady State Versus Steady State

The differences between dynamic-steady state and steady state are evident in the normalized salt mass (Figure 2). Tides and repeated surges (Figures 2a and 2b) cause a long-term increase in the salt mass from the steady-state value, such that the dynamic steady states yield salt masses that are 60% and 15% higher than those simulated with a constant SL for tides and surges, respectively. For the larger-scale, glacial-cycle simulations, the fluctuations in salinity were in-phase with the fluctuations in SL, meaning that in this unconfined system the salinity distribution responds quickly enough to equilibrate with the instantaneous SL. Accordingly, the average salinity distribution was similar between the steady state with average SL and the average salinity distribution with cyclical forcing. However, the salt mass fluctuates such that its maximum value is ~20% greater than the salt mass simulated in steady state with the maximum SL (Figure 2c). When SL drops, the salt flushes out and the salt mass in the aquifer drops to a minimum of ~80% lower than the steady-state salt mass (Figure 2c). In the tidal simulation, there is a slight decrease in the salt mass after 60 years (Figure 2a), which is likely related to a large-scale rebound effect of the fluctuations, such that the transition zone temporarily reaches further inland than its final location (Morgan et al., 2013, 2015).

In all simulated processes, substantial differences were observed in the location of the mixing zone compared with the steady-state simulation with constant SL (Figure 3). Importantly, these differences were observed when the simulated SL was at its average (tides) or present-day (storms, glacial cycles) elevation (black circles in Figures 1 and 2). This implies that the assumption of steady state (simulated by holding the SL constant at its present elevation) potentially creates substantial errors in the salinity distribution of the aquifer. For the high-frequency fluctuations (tides and surges), these differences were persistent and the time-averaged salinity distributions in dynamic steady state were different from the steady salinity distribution using average or present conditions. For the tidal simulations, in the transient case, the mixing zone was slightly wider and its center was shifted ~400 m

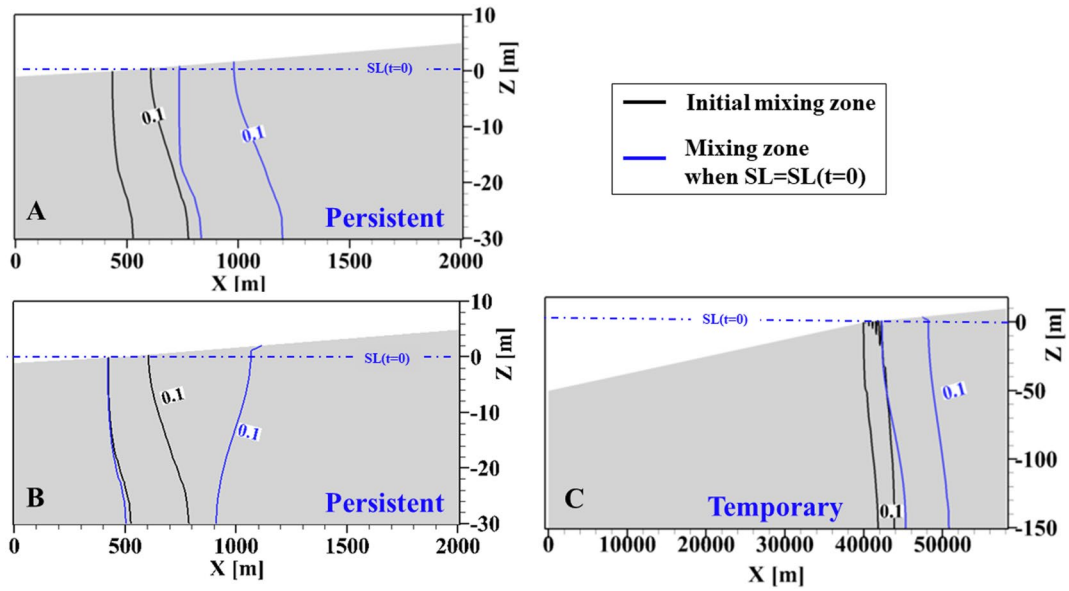

Figure 3. The distribution of the mixing zone in steady-state conditions (black) and for transient conditions (blue), delineated by the $C = 0.1$ (labeled) and the $C = 0.9$ contours. Transient mixing zones are plotted for the different cyclical processes: (a) Tides; (b) Surges; (c) Glacial fluctuations in sea level (SL). See black circles in Figures 1 and 2 for the times for which the blue contours (transient mixing zones) are plotted. For the tides (a) and surges (b) this transient transition zone was persistent, but for the glacial cycles (c) the transition zone changed when the SL boundary condition changed.

inland compared to the steady-state case. For the storm-surge simulations, the 0.9 salinity contours were co-located for the steady-state and transient cases while the 0.1 salinity contour was shifted substantially inland. For the glacial simulation, the mixing zone was wider in the transient simulation and its center reached further inland compared with the steady state, but this difference was temporary.

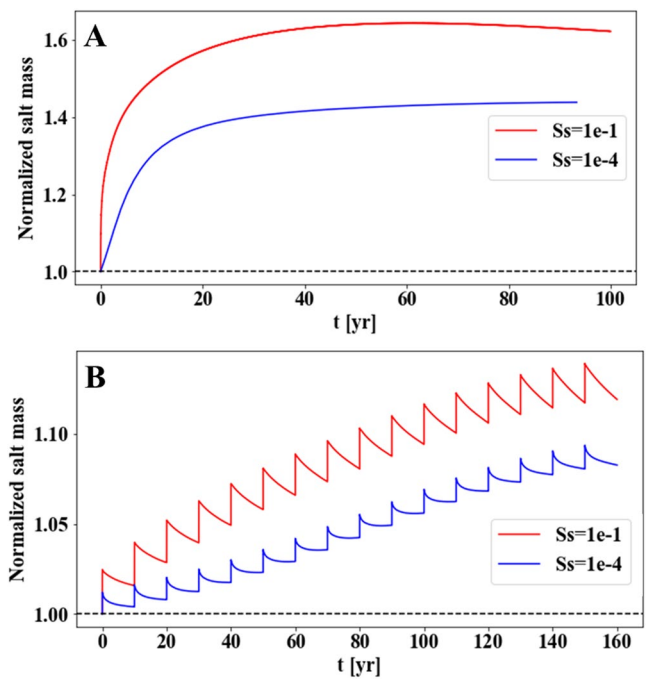

Figure 4. Normalized salt mass ($\overline{SM}$) in the aquifer for different values of specific storage (S_s) under (a) tides and (b) repetitive surges. Black dashed lines mark the initial (steady state) value.

3.2. The Effect of Aquifer Storativity

One of the hydrologic characteristics that is widely considered as unimportant for predicting long-term average salinity distributions in coastal aquifers is the aquifer storativity (S). The long- and short-term impacts of cyclical processes on the dynamic steady state of coastal aquifers (Figures 2 and 3) suggest that storativity may play a role in dictating modern-day average salinity, even without considering other transient alterations to the flow regime (e.g., pumping, seasonality). For the simulations that showed a long-term effect on the salt mass stored in the aquifer (tides and surges, Figures 2a and 2b), the deviation from steady-state salinity depended strongly on the value of S (Figure 4). The response of aquifers to hydrologic shifts is controlled by the hydraulic diffusivity (D_a), defined as the hydraulic conductivity (K) times the aquifer thickness (b) over the storativity (S):

$$D_a = \frac{Kb}{S} \tag{2}$$

According to Equation 2, the hydraulic diffusivity of the aquifer is inversely proportional to its storativity. Indeed, we find that higher S (lower diffusivity) yields a higher long-term impact due to the less efficient dissipation of the forcing (slower aquifer recovery). Thus, the salt mass that is vertically added to the aquifer in the long term is smaller for lower S (higher diffusivity) because the response is faster and the added salt is more readily flushed out

(Figure 4). The hydraulic diffusivity is also dependent on the hydraulic conductivity (K), which was not changed here to ensure a consistent steady state without cyclical forcings.

4. Discussion and Conclusions

The results of this work demonstrate that cyclical processes control the salinity distributions in coastal aquifers over multiple spatio-temporal scales. High-frequency fluctuations in SL (tides and repetitive surges) have a persistent effect on the salinity, such that there is a significant, long-term shift in the average salinity in the aquifer (Figure 2, a&b). This persistent effect on the average salinity occurs because the response time of the aquifer is longer than the time scale of the fluctuations, and the aquifer does not recover between peaks in SL. Paldor and Michael (2021) formulated a non-dimensional characteristic time (denoted τ') to relate these two time scales through the hydraulic diffusivity (D_a, Equation 2) of the aquifer:

$$\tau' = \frac{L^2}{D_a T} \tag{3}$$

In Equation 3, T is the period of the forcing, and L is a characteristic length, typically taken as the thickness of the aquifer. Using the relationship in Equation 3, Paldor and Michael (2021) showed that higher hydraulic diffusivities reduce the long-term impact of repetitive storm surges. Here we show that high-frequency (low T) processes in general (waves, tides, storms) are potentially responsible for discrepancies between observed average salinities and salinities estimated based on steady-state assumptions. Low-frequency processes such as glacial cycles do not have a long-term impact on the average salinity (Figure 2c), as predicted by Equation 3 (higher T yields lower τ'). Previous models and physical experiments showed that tidal fluctuations may push the interface seaward (Kuan et al., 2012), which is the opposite of our finding. However, in the models and experiments conducted by Kuan et al. (2012), an upper saline plume developed. In our model there is no upper saline plume due to the low K (5 md^{-1}) (Evans & Wilson, 2016). The salt added at the top initially pushes the transition zone seaward, but the long-term effect is a more landward extent of the transition zone, as simulated here and by Paldor and Michael (2021).

We further show that while they do not necessarily alter the average salinity, low-frequency changes in SL may induce inconsistencies between estimated and actual present-day salinities, because systems are still responding to longer-term forcings, even without considering shorter-scale fluctuations. For example, the simulated response to interglacial SL rise dictates a mixing zone that is further inland at the maximum SL than that simulated with a steady SL at the maximum value (Figure 3c). The snapshot of the mixing zone (blue contours in Figure 3c) is when the simulated SL is at its initial location, which is the steady-state SL. This means that estimates of present-day salinity distributions that are based on steady-state assumptions likely underestimate the inland extent of the mixing zone. This difference occurs due to an "overshoot effect," wherein sea-level rise causes inland movement of the subsurface transition zone to temporarily exceed its final location. This effect was previously simulated numerically and observed in physical experiments on smaller spatio-temporal scales (Morgan et al., 2013; Stoeckl et al., 2019; Walther et al., 2020; Watson et al., 2010). Here we show that when considering the large-scale fluctuations due to glacial cycles, the overshoot of the transition zone potentially introduces significant discrepancies and should be considered in studies that aim to estimate the distribution of salt in coastal aquifers. We note that these results are for unconfined aquifers that are fully connected to the ocean boundary. In systems with confining units that impede the connection, response times may be much slower, leading to stronger differences between instantaneous and average conditions, and potentially creating differences between steady state and dynamic steady state that are similar to those for higher frequency fluctuations (Gustafson et al., 2019; Haroon et al., 2021; Micallef et al., 2020; Michael et al., 2016; Paldor et al., 2020). Similarly, the impeded connection may mute the effects of higher-frequency fluctuations.

In many hydrogeologic studies of coastal systems, the aim is to calibrate a groundwater flow and salt transport model based on field observations. The most common practice in such studies is to run a steady-state simulation of the studied area, with the model parameters adapted to match the modeled steady state to the observed average state of the aquifer. The output of the calibrated steady-state model is applied as initial conditions for transient simulations (which may or may not include cyclical processes), which are used to constrain the dominant factors that control the hydrologic functioning of a given system (Fang et al., 2021; Levanon et al., 2016; Oz et al., 2015; Paldor et al., 2019). Transient simulations are also used to assess vulnerability to various environmental changes (e.g., sea-level rise, recharge intensification), and to predict future trends in the hydrologic regime (Guimond &

Michael, 2021; Masterson et al., 2014; Paldor & Michael, 2021; Xiao et al., 2018). This approach assumes that the steady state of the aquifer is reflected in the calibration targets, which are commonly the observed long-term averaged heads and salinities. Such an assumption can lead to erroneous initial conditions and calibrated parameter values which could potentially invalidate transient simulations and long-term predictions based on them. One aquifer parameter that is commonly ignored in the calibration of numerical models is the storativity which measures an aquifer's response to changes in the hydraulic regime, and therefore drops out of the steady-state groundwater flow equation. This is a common approach in hydrogeologic modeling, and our findings suggest that a paradigm shift may be needed, as storativity likely plays an important role in dictating the average salinities when considering relatively high-frequency (i.e., high τ') cyclical forcings. This suggested paradigm shift raises an important question regarding the spin-up time required in hydrogeologic modeling. This depends on the specific modeled problem, since it is often unfeasible to run models for glacial time scales. Balancing model accuracies and reliabilities with feasible runtimes is a major challenge in hydrogeologic modeling, and this study suggests that net effects of cyclical processes should also be considered when deciding on the approach for specific problems.

The simulated values of specific storage in this study are not necessarily representative of actual aquifers (Domenico & Mifflin, 1965). However, the adopted values mimic changes in the overall storativity of the aquifer, where unconfined aquifers typically have significantly higher storativities than confined ones due to the specific yield. Our results indicate that unconfined aquifers may be more prone to the long-term impact of high-frequency forcings (Figure 4). Since unconfined aquifers typically generate coastal submarine groundwater discharge (SGD), the importance of our findings span beyond the matter of water resources management. Coastal SGD is responsible for nutrient supply and sustains ecosystems in many coastal environments (Moore, 2010). Therefore, studies monitoring changes in coastal ecosystems should consider the possibility that offshore biogeochemical inputs and hot spots (specific locations that are highly reactive or rich in nutrients) are shifting along with the aquifer's continued response to past changes, not necessarily due to present-day changes. Further exploration of this effect is beyond the scope of the present study, and it is suggested here merely as a potential implication of the hydrogeological effect of multi-scale cyclical changes in SL.

This study has important implications for water resources. We show that salinity may be permanently elevated much further inland than predicted by average SL due to even seemingly minor cyclical sea-level variations such as diurnal tides or ocean surges. Because salinity distributions in coastal aquifers are difficult to observe directly, coastal hydrogeologists rely heavily on models to guide groundwater resources management. Our results show that the typical model simplification of neglecting cyclical processes that operate on vastly different timescales than that of interest could invalidate both our initial conditions and our calibrated parameters. Thus, water managers and modelers must consider the net effect of cyclical changes on particular aquifer systems by considering the period and amplitude of cyclical change relative to the size and hydrogeologic characteristics of the aquifer system to avoid potentially large-scale errors in predictions of the current state and future evolution of precious coastal water resources.

Data Availability Statement

No data are used in this manuscript.

Acknowledgments
This research was funded by the US National Science Foundation (OCE184865 and OIA1757353) and the US Geological Survey (NIWR/USGS 2018DE01G).

References

Chang, S. W., Clement, T. P., Simpson, M. J., & Lee, K. K. (2011). Does sea-level rise have an impact on saltwater intrusion? *Advances in Water Resources*, *34*(10), 1283–1291. https://doi.org/10.1016/j.advwatres.2011.06.006

Cohen, D., Person, M., Wang, P., Gable, C. W., Hutchinson, D., Marksamer, A., et al. (2010). Origin and extent of fresh paleowaters on the Atlantic continental shelf, USA. *Ground Water*, *48*(1), 143–158. https://doi.org/10.1111/j.1745-6584.2009.00627.x

Domenico, P. A., & Mifflin, M. D. (1965). Water from low-permeability sediments and land subsidence. *Water Resources Research*, *1*(4), 563–576. https://doi.org/10.1029/WR001i004p00563

Evans, T. B., & Wilson, A. M. (2016). Groundwater transport and the freshwater-saltwater interface below sandy beaches. *Journal of Hydrology*, *538*, 563–573. https://doi.org/10.1016/j.jhydrol.2016.04.014

Fang, Y., Zheng, T., Zheng, X., Yang, H., Wang, H., & Walther, M. (2021). Influence of tide-induced unstable flow on seawater intrusion and submarine groundwater discharge. *Water Resources Research*, *57*(4), e2020WR029038. https://doi.org/10.1029/2020WR029038

Guimond, J. A., & Michael, H. A. (2021). Effects of marsh migration on flooding, saltwater intrusion, and crop yield in coastal agricultural land subject to storm surge inundation. *Water Resources Research*, *57*(2). https://doi.org/10.1029/2020WR028326

Gustafson, C., Key, K., & Evans, R. L. (2019). Aquifer systems extending far offshore on the U.S. Atlantic margin. *Scientific Reports*, *9*(1), 8709. https://doi.org/10.1038/s41598-019-44611-7

Haroon, A., Micallef, A., Jegen, M., Schwalenberg, K., Karstens, J., Berndt, C., et al. (2021). Electrical resistivity anomalies offshore a carbonate coastline: Evidence for freshened groundwater? *Geophysical Research Letters*, *48*(14), e2020GL091909. https://doi.org/10.1029/2020GL091909

Kuan, W. K., Jin, G., Xin, P., Robinson, C., Gibbes, B., & Li, L. (2012). Tidal influence on seawater intrusion in unconfined coastal aquifers. *Water Resources Research*, *48*(2). https://doi.org/10.1029/2011WR010678

Levanon, E., Shalev, E., Yechieli, Y., & Gvirtzman, H. (2016). Fluctuations of fresh-saline water interface and of water table induced by sea tides in unconfined aquifers. *Advances in Water Resources*, *96*, 34–42. https://doi.org/10.1016/J.ADVWATRES.2016.06.013

Levanon, E., Yechieli, Y., Gvirtzman, H., & Shalev, E. (2017). Tide-induced fluctuations of salinity and groundwater level in unconfined aquifers – Field measurements and numerical model. *Journal of Hydrology*, *551*, 665–675. https://doi.org/10.1016/j.jhydrol.2016.12.045

Masterson, J. P., Fienen, M. N., Thieler, E. R., Gesch, D. B., Gutierrez, B. T., & Plant, N. G. (2014). Effects of sea-level rise on barrier island groundwater system dynamics – Ecohydrological implications. *Ecohydrology*, *7*(3), 1064–1071. https://doi.org/10.1002/ECO.1442

Micallef, A., Person, M., Haroon, A., Weymer, B. A., Jegen, M., Schwalenberg, K., et al. (2020). 3D characterisation and quantification of an offshore freshened groundwater system in the Canterbury Bight. *Nature Communications*, *11*(1), 1372. https://doi.org/10.1038/s41467-020-14770-7

Michael, H. A., Post, V. E. A., Wilson, A. M., & Werner, A. D. (2017). Science, society, and the coastal groundwater squeeze. *Water Resources Research*, *53*(4), 2610–2617. https://doi.org/10.1002/2017WR020851

Michael, H. A., Scott, K. C., Koneshloo, M., Yu, X., Khan, M. R., & Li, K. (2016). Geologic influence on groundwater salinity drives large seawater circulation through the continental shelf. *Geophysical Research Letters*, *43*(20), 10782–10791. https://doi.org/10.1002/2016GL070863

Moore, W. S. (2010). The effect of submarine groundwater discharge on the ocean. *Annual Review of Marine Science*, *2*(1), 59–88. https://doi.org/10.1146/annurev-marine-120308-081019

Morgan, L. K., Bakker, M., & Werner, A. D. (2015). Occurrence of seawater intrusion overshoot. *Water Resources Research*, *51*(4), 1989–1999. https://doi.org/10.1002/2014WR016329

Morgan, L. K., Stoeckl, L., Werner, A. D., & Post, V. E. A. (2013). An assessment of seawater intrusion overshoot using physical and numerical modeling. *Water Resources Research*, *49*(10), 6522–6526. https://doi.org/10.1002/wrcr.20526

Nielsen, P. (1999). Groundwater dynamics and salinity in coastal barriers. *Journal of Coastal Research*, *15*(3), 732–740.

Oz, I., Shalev, E., Yechieli, Y., & Gvirtzman, H. (2015). Saltwater circulation patterns within the freshwater-saltwater interface in coastal aquifers: Laboratory experiments and numerical modeling. *Journal of Hydrology*, *530*, 734–741. https://doi.org/10.1016/j.jhydrol.2015.10.033

Paldor, A., Aharonov, E., & Katz, O. (2020). Thermo-haline circulations in subsea confined aquifers produce saline, steady-state deep submarine groundwater discharge. *Journal of Hydrology*, *580*, 124276. https://doi.org/10.1016/j.jhydrol.2019.124276

Paldor, A., & Michael, H. A. (2021). Storm surges cause simultaneous salinization and freshening of coastal aquifers, exacerbated by climate change. *Water Resources Research*, *57*(5), e2020WR029213. https://doi.org/10.1029/2020WR029213

Paldor, A., Shalev, E., Katz, O., & Aharonov, E. (2019). Dynamics of saltwater intrusion and submarine groundwater discharge in confined coastal aquifers: A case study in northern Israel. *Hydrogeology Journal*, *27*(5), 1611–1625. https://doi.org/10.1007/s10040-019-01958-5

Person, M., Dugan, B., Swenson, J. B., Urbano, L., Stott, C., Taylor, J., & Willett, M. (2003). Pleistocene hydrogeology of the Atlantic continental shelf, New England. *Bulletin of the Geological Society of America*, *115*(11), 1324–1343. https://doi.org/10.1130/B25285.1

Post, V. E. A., Groen, J., Kooi, H., Person, M., Ge, S., & Edmunds, W. M. (2013). Offshore fresh groundwater reserves as a global phenomenon. *Nature*, *504*(7478), 71–78. https://doi.org/10.1038/nature12858

Robinson, C., Li, L., & Barry, D. A. (2007). Effect of tidal forcing on a subterranean estuary. *Advances in Water Resources*, *30*(4), 851–865. https://doi.org/10.1016/j.advwatres.2006.07.006

Stoeckl, L., Walther, M., & Morgan, L. K. (2019). Physical and numerical modelling of post-pumping seawater intrusion. *Geofluids*, 1–11. https://doi.org/10.1155/2019/7191370

Tebaldi, C., Strauss, B. H., & Zervas, C. E. (2012). Modelling sea level rise impacts on storm surges along US coasts. *Environmental Research Letters*, *7*(1), 014032. https://doi.org/10.1088/1748-9326/7/1/014032

Therrien, R., McLaren, R. G., Sudicky, E. A., & Panday, S. M. (2010). HydroGeoSphere. A three-dimensional numerical model describing fully-integrated subsurface and surface flow and solute transport. In *Groundwater Simulations Group*. https://doi.org/10.5123/S1679-49742014000300002

Walther, M., Stoeckl, L., & Morgan, L. K. (2020). Post-pumping seawater intrusion at the field scale: Implications for coastal aquifer management. *Advances in Water Resources*, *138*, 103561. https://doi.org/10.1016/j.advwatres.2020.103561

Watson, T. A., Werner, A. D., & Simmons, C. T. (2010). Transience of seawater intrusion in response to sea level rise. *Water Resources Research*, *46*(12). https://doi.org/10.1029/2010WR009564

Xiao, H., Wang, D., Medeiros, S. C., Hagen, S. C., & Hall, C. R. (2018). Assessing sea-level rise impact on saltwater intrusion into the root zone of a geo-typical area in coastal east-central Florida. *Science of The Total Environment*, *630*, 211–221. https://doi.org/10.1016/J.SCITOTENV.2018.02.184

Xin, P., Robinson, C., Li, L., Barry, D. A., & Bakhtyar, R. (2010). Effects of wave forcing on a subterranean estuary. *Water Resources Research*, *46*(12), 12505. https://doi.org/10.1029/2010WR009632

Xu, Z., Hu, B. X., & Ye, M. (2018). Numerical modeling and sensitivity analysis of seawater intrusion in a dual-permeability coastal karst aquifer with conduit networks. *Hydrology and Earth System Sciences*, *22*(1), 221–239. https://doi.org/10.5194/hess-22-221-2018